

High-Resolution Cortical Dipole Layer Imaging Based on Noise Covariance Matrix

Junichi Hori, *Senior Member* and Satoru Watanabe, *Nonmember, IEEE*

Abstract—We have investigated the suitable spatial filters for inverse estimation of cortical dipole imaging from the scalp electroencephalogram. The effects of incorporating statistical information of noise into inverse procedures were examined by computer simulations and experimental studies. The parametric projection filter (PPF) was applied to an inhomogeneous three-sphere volume conductor head model. The noise covariance matrix was estimated by applying independent component analysis (ICA) to the scalp potentials. Moreover, the sampling method of the noise information was examined for calculating the noise covariance matrix. The simulation results suggest that the spatial resolution was improved while the effect of noise was suppressed by including the separated noise at the time instant of imaging and by adjusting the number of samples according to the signal to noise ratio.

I. INTRODUCTION

ELECTROENCEPHALOGRAPHY (EEG) has been a useful modality to provide high temporal resolution of underlying brain electrical activity. However the spatial resolution of EEG is limited due to the smearing effect of the head volume conductor. Equivalent dipole imaging has been proposed to estimate the high-resolution cortical dipole layer (DL) distribution to account for the scalp potential (SP) [1]-[8]. DL imaging provides the advantage that high-resolution brain electrical activity can be estimated without an ad hoc assumption about the number of source dipoles. We have developed an inverse procedure for cortical dipole source imaging using a parametric projection filter (PPF) which enables estimation of inverse solutions in the presence of noise information [9], [10]. Information related to noise distribution, as defined by the covariance matrix, is assumed to be known. Our previous results indicated that the PPF provides a better approximation to the original DL distribution than that of traditional inverse techniques in the case of low correlation between signal and noise distributions. Moreover, Wiener reconstruction frameworks based on both signal and noise covariance matrices have been also investigated [2], [11]-[15].

In fact, the signal and noise information are unknown in EEG measurements. However, in order to realize high-resolution brain functional imaging, it is necessary to estimate signal and noise components. In this study, the noise covariance matrix was estimated from the noise components

which were separated by applying independent component analysis (ICA) to the original EEG signals. Moreover, the sampling method of the noise information was examined for calculating noise covariance. We investigated the performance of these inverse filters by computer simulations and human experimental studies.

II. METHOD

A. Cortical Dipole Imaging

In the cortical dipole imaging study, the head volume conductor was approximated by the inhomogeneous three-concentric sphere model [6]. This model incorporates variation in conductivity of different tissues such as the scalp, the skull, and the brain; it has been used to provide a reasonable approximation to head volume conductor for cortical imaging. An equivalent DL within the brain simulates the brain electrical activity. The transfer matrix from the DL to the SP is obtained by considering the geometry of the model and the physical relationships among the quantities involved. The DL distribution is reconstructed from the recorded SP by solving an inverse problem of the transfer matrix.

The observation system of brain electrical activity on the scalp surface is defined using the following equation:

$$\mathbf{g} = \mathbf{A} \mathbf{f} + \mathbf{n} \quad (1)$$

where \mathbf{f} is the vector of the equivalent dipole sources distributed over the DL, \mathbf{n} is the additive noise, and \mathbf{g} is the SP. In addition, \mathbf{A} represents the transfer matrix from the equivalent dipole sources to the SP signals. It is important to infer the origins from the recorded EEG and to map the sources that generate the scalp EEG. Thus, the inverse problem is defined as

$$\mathbf{f}_0 = \mathbf{B} \mathbf{g} \quad (2)$$

where \mathbf{B} is the inverse filter from the scalp EEG to the DL distribution and \mathbf{f}_0 is the estimated source distribution of the DL. Because the number of measurement electrodes is always much smaller than the dimensions of the unknown vector \mathbf{f} , this problem is an underdetermined inverse problem.

B. Spatial Inverse Filter

Several inverse techniques have been proposed to solve such inverse problems. In the presence of noise, the truncated singular value decomposition [16] or Tikhonov regularization

Manuscript received April 7, 2009. This work was supported in part by NS Promotion Foundation for Science of Perception.

J. Hori and S. Watanabe are with the Department of Biocybernetics, Niigata University, Niigata 950-2181 Japan (phone: 81-25-262-6733; fax: 81-25-262-7010; e-mail: hori@eng.niigata-u.ac.jp).

method [17] can be used to calculate the pseudo inverse filter.

The parametric projection filter (PPF), which allows estimating solutions in presence of information on noise covariance structure, has been introduced to solve the inverse problem [9], [10]. The PPF is given by

$$\mathbf{B} = \mathbf{A}^T (\mathbf{A}\mathbf{A}^T + \gamma \mathbf{Q})^{-1} \quad (3)$$

where γ is a small positive number known as the regularization parameter and \mathbf{A}^T the transpose matrix of \mathbf{A} . The regularization parameter γ determines the restorative ability. The determination of the value of parameter γ is left to the subjective judgment of the user. We have developed a criterion that estimates the optimum parameter using iterative calculation for restoration [9]. The criterion estimates the parameter that minimizes the approximated error between the original and estimated source signals without knowing the original source distribution.

The matrix \mathbf{Q} is the noise covariance derived from the expectation over the noise ensemble $E[\mathbf{n} \mathbf{n}^T]$. Actually, each component of the matrix \mathbf{Q} is approximated from

$$Q_{i,j} = \frac{1}{K} \sum_{k=1}^K (n_{k,i} - \mu_i)(n_{k,j} - \mu_j) \quad (4)$$

$(i, j = 1, 2, \dots, J)$

where J is the number of electrodes and K is the number of observations of sampled noise. In a clinical and experimental setting, the noise covariance \mathbf{Q} might be estimated from data that are known to be source-free, such as pre-stimulus data in evoked potentials [11]. However, it was difficult to distinguish the noise from EEG data. In the present study, we estimate the noise covariance using ICA as described in next section.

C. Independent Component Analysis

The PPF in (3) requires the noise covariance. However, the signal and noise components are intermingled in the observed EEG signals. In such cases, each component was separated by ICA, which extracts independent sources from the observed signal based on statistical independence of the original signal. The FastICA algorithm was used for performing the estimation of ICA [18]. This algorithm is based on a fixed-point iteration scheme maximizing non-Gaussianity as a measure of statistical independence. Non-Gaussianity was measured using an approximation of negentropy. The outline of ICA algorithm is as follows:

When independent sources \mathbf{s} are mutually mixed by a mixing matrix \mathbf{M} , the observed signal \mathbf{g} is described by

$$\mathbf{g} = \mathbf{M} \mathbf{s} \quad (5)$$

First, the number of sources is decided using principal component analysis (PCA). The principal component \mathbf{z} is expressed as

$$\mathbf{z} = \mathbf{V} \mathbf{g} \quad (6)$$

where \mathbf{V} is the whitening matrix. Actually, \mathbf{V} serves to reduce the dimensionality of the matrix. Next, independent signals are estimated using the appropriate restoring matrix \mathbf{W} . Finally, the original signal is estimated as

$$\mathbf{s}_0 = \mathbf{W} \mathbf{z} \quad (7)$$

That is, an inverse of the mixing matrix \mathbf{M} is described by multiplying a whitening matrix \mathbf{V} and a restoring matrix \mathbf{W} ($\mathbf{M}^{-1} = \mathbf{W} \mathbf{V}$).

ICA was applied to EEG signals, and the independent components were extracted. These components were separated into the signal and the noise components according to the a priori anatomical information. Thus, we obtained the separated signal and noise by applying a mixing matrix. The noise covariance matrix was estimated from the differential noise between the original EEG signal and separated signal. Finally, the space inverse filter was designed using this noise covariance matrix for high resolution cortical dipole imaging.

D. Simulation

In the present simulation study, single dipole source was used to represent the spatial resolution of the brain electrical activity. The dipole was oriented radially to the sphere with varying strengths. The eccentricity of the source was set as 0.7. The strength of the dipole changed as the damped oscillation with the frequency of 13 Hz giving the evoked potentials or the event-related potentials (Fig. 1(a)). Data was collected for 0.4 s with a sampling of 100 Hz.

In the inhomogeneous spherical source-conductor model [6], [11], the radii of the brain, the skull, and the scalp spheres were set to 0.87, 0.92, and 1.0, respectively [6]. The normalized conductivity of the scalp and the brain were set to $\sigma_0 = 1.0$, and that of the skull to $\sigma_s = 0.0125$. The potentials on the scalp surface, generated by current dipoles inside the brain, can be calculated by solving the forward problem from the dipole source to the scalp-surface potential. The scalp potentials were contaminated with 5-20% Gaussian white noise (GWN). The strength of the DL distribution can be calculated by solving the forward problem from the assumed dipole source to the equivalent DL strength. A DL with 1280 radial dipoles at a radius of 0.8 was used. We compared the ability of spatial inverse filters constructed with various noise conditions. We evaluated the estimating abilities using the relative error between actual and estimated DL distributions and maps of estimated cortical DL imaging.

III. RESULTS

We compared the estimation results when the noise covariance of the PPF was calculated with various conditions. Fig. 1(b) shows the separated signal components with ICA. Fig. 1(c) shows the differential noise components between the measured EEG and separated noise components which is

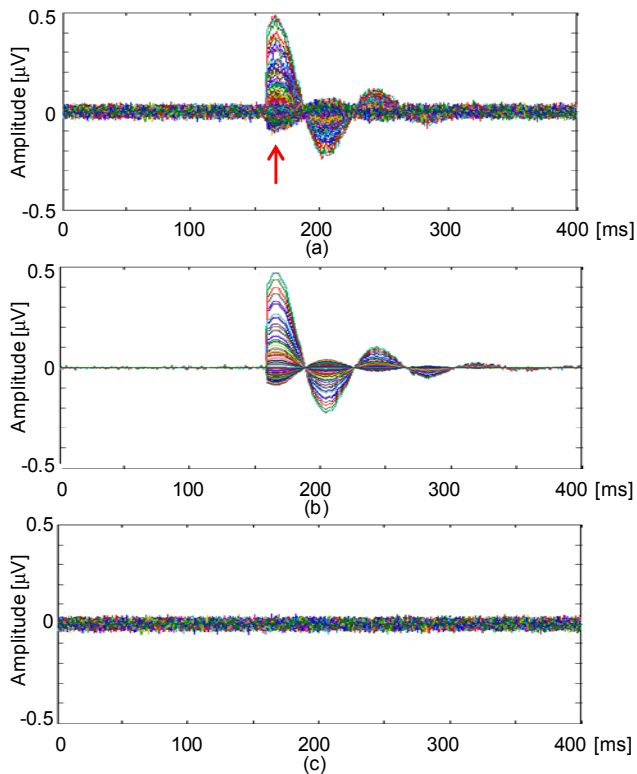


Fig.1. Example of the simulated EEG signals. (a) Simulated EEG signals contaminated with 10% GWN. (b) Separated signal components with ICA. (c) Differential noise components between (a) and (b).

similar to the actual noise components. Figure 2 shows simulation results of relative error between the actual and estimated cortical maps ($\frac{\|f-f_0\|}{\|f\|}$) against the time instant of noise. The dipole imaging was carried out at the time point of 165ms that was peak of EEG signal in Fig.1 (a). The noise level was 0.1. The time interval of noise was 80ms. When the time interval of noise samples included the imaging time instant, the relative errors were dramatically reduced to 0.6. We confirmed that the estimated cortical maps were also improved.

Figure 3 shows simulation results of the relative error between the actual and estimated cortical maps against the sampling number of noise. The dipole imaging was carried out at the time point of 165ms. The noise was sampled including the time instant of imaging. The optimum sampling numbers changed according to the noise level (NL) of the scalp potential. When the EEG signals are noisy in clinical measurements, the relative error can be reduced by increasing the sampling number.

Figure 4 shows examples of the estimated inverse solutions of cortical dipole imaging for visual evoked potential (VEP). The maps shows the dipole layer distributions observed from the back of the head. Figure 4 (a)-(e) show estimated cortical dipole imaging using the PPF. \mathbf{Q} was calculated from the separated noise of (a) $K=10$, (b) $K=20$, (c) $K=30$, and (d) $K=40$ samples. In Fig.4 (e), \mathbf{Q} was calculated from pre-stimulus data. As compared with the scalp potential in Fig.4 (f), the estimated dipole imaging performed well.

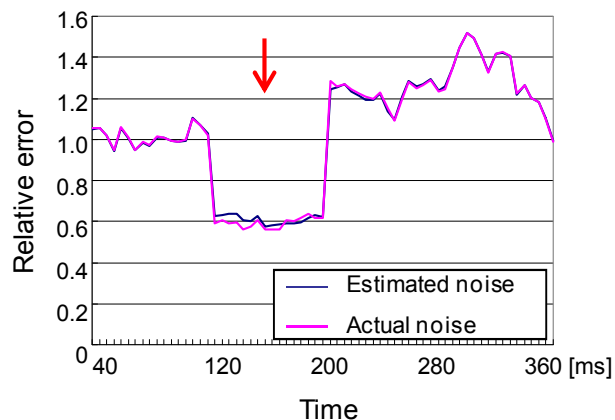


Fig. 2. Simulation results of relative error between actual and estimated cortical maps against the time instant of noise. The dipole imaging was carried out at the time point of 165ms with a noise level of 0.1 and a time interval of noise of 80ms.

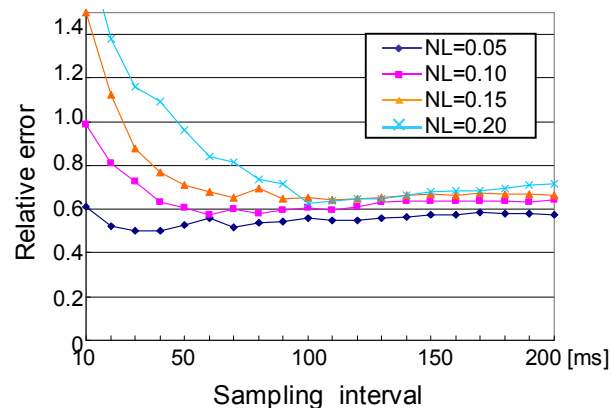


Fig. 3. Simulation results of relative error between actual and estimated cortical maps against the time interval of noise. The dipole imaging was carried out at the time point of 165ms. The noise was sampled including the time instant of imaging.

Especially, when the \mathbf{Q} was estimated with 20 noise samples, the maps demonstrated the localized area around the visual field with less noise.

IV. DISCUSSION

We considered improving the precision of cortical dipole imaging by applying spatial inverse filters incorporated with statistical information of noise. We examined new estimation methods of the noise covariance matrix for equivalent cortical dipole imaging using the PPF. The noise component was extracted from EEG signals using ICA. It was better to use differential noise for calculating noise covariance in PPF rather than separated noise. In the FastICA algorithm, PCA was used for reducing the dimension of the signals. Therefore, most of the noise components might be lost when separating noise.

In this paper, we investigated the method of acquiring the

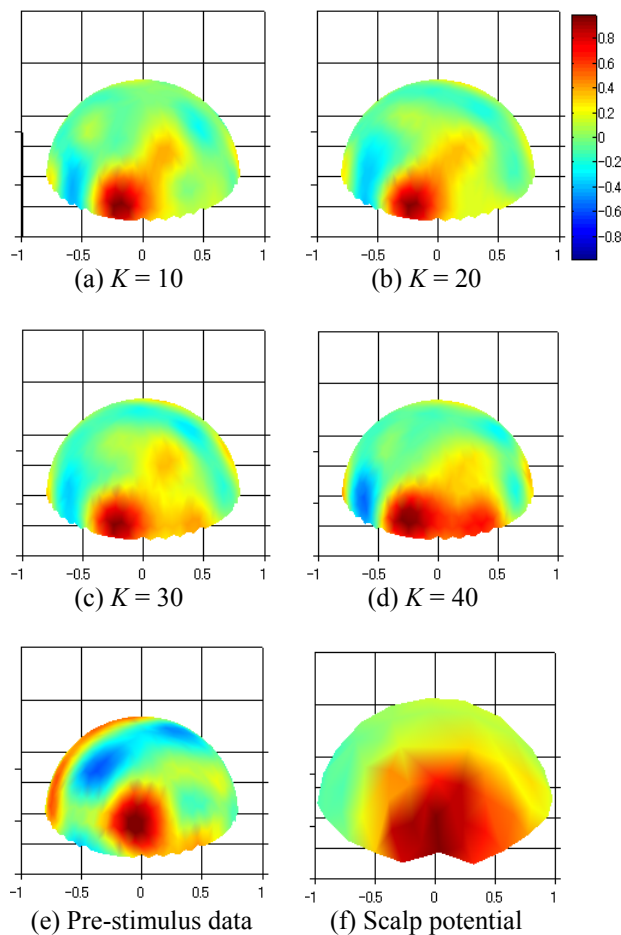


Fig. 4. Examples of the estimated inverse solutions of cortical dipole imaging for VEP. (a)-(e) Estimated cortical dipole imaging using PPF. \mathbf{Q} was calculated from the separated noise of (a) $K=10$, (b) $K=20$, (c) $K=30$, and (d) $K=40$ samples. (e) \mathbf{Q} was calculated from pre-stimulus data. (f) Scalp potential.

noise data in order to calculate the noise covariance matrix \mathbf{Q} built in the PPF by the computer simulation. As a result, it was confirmed that the accuracy was improved by calculating \mathbf{Q} by containing noise information to the time point of the dipole imaging. Moreover, it has been understood that the estimated maps were localized by adjusting the time interval of noise according to the signal to noise ratio.

In addition, the proposed method was applied to clinical data based on the above-mentioned results. In this case, when the time interval of noise was set to $K = 40$ ms for calculating \mathbf{Q} , the DL distribution was blurred. On the other hand, when $K = 10$ ms or 20 ms, the peak of the DL distribution was well-localized while the noise was reduced. The obtained result was in good agreement with a physiological knowledge. These results suggest that the noise components obtained from ICA can be used for noise covariance estimation.

Further investigations using a more realistic head conductor model and experimental data are necessary to validate the performance of the proposed model in cortical dipole source localization.

REFERENCES

- [1] R. Sidman, M. Ford, G. Ramsey, and C. Schlichting, "Age-related features of the resting and P300 auditory evoked responses using the dipole localization method and cortical imaging technique," *J. Neurosci. Meth.*, vol. 33, pp. 23-32, 1990.
- [2] R. Srebro, R. M. Oguz, K. Hughlett, and P. D. Purdy, "Estimating regional brain activity from evoked potential field on the scalp," *IEEE Trans. Biomed. Eng.*, vol. 40, pp. 509-516, 1993.
- [3] A. Gevins, J. Le, N. K. Martin, P. Brickett, J. Desmond, and B. Reutter, "High resolution EEG: 124-channel recording, spatial deblurring and MRI integration methods," *Electroenceph. Clin. Neurophysiol.*, vol. 90, pp. 337-358, 1994.
- [4] P. Nunez, R. B. Silibertein, P. J. Cdush, R. S. Wijesinghe, A. F. Westdrop, and R. Srinivasan, "A theoretical and experimental study of high resolution EEG based on surface Laplacian and cortical imaging," *Electroenceph. Clin. Neurophysiol.*, vol. 90, pp. 40-57, 1994.
- [5] F. Babiloni, C. Babiloni, F. Carducci, L. Fattorini, C. Anello, P. Onorati, and A. Urbano, "High resolution EEG: a new model-dependent spatial deblurring method using a realistically-shaped MR-constructed subject's head model," *Electroenceph. Clin. Neurophysiol.*, vol. 102, pp. 69-80, 1997.
- [6] Y. Wang and B. He, "A computer simulation study of cortical imaging from scalp potentials," *IEEE Trans. Biomed. Eng.*, vol. 45, pp. 724-735, 1998.
- [7] G. Edlinger, P. Wach, and G. Pfurtscheller, "On the realization of an analytic high-resolution EEG," *IEEE Trans. Biomed. Eng.*, vol. 45, pp. 736-745, 1998.
- [8] B. He, Y. Wang, and D. Wu, "Estimating cortical potentials from scalp EEG's in a realistically shaped inhomogeneous head model," *IEEE Trans. Biomed. Eng.*, vol. 46, pp. 1264-1268, 1999.
- [9] J. Hori and B. He, "Equivalent dipole source imaging of brain electric activity by means of parametric projection filter," *Annals Biomed. Eng.*, vol. 29, pp. 436-445, 2001.
- [10] J. Hori, M. Aiba, and B. He, "Spatio-temporal dipole source imaging of brain electrical activity by means of time-varying parametric projection filter," *IEEE Trans. Biomed. Eng.*, vol.51, no.5, pp.768-777, May 2004.
- [11] A. M. Dale and M. I. Sereno, "Improved localization of cortical activity by combining EEG and MEG with MRI cortical surface reconstruction: a linear approach," *J. Cognitive Neuroscience*, vol. 5, pp. 162-176, 1993.
- [12] J. W. Philips, R. M. Leahy, and J. C. Mosher, "MEG-based imaging of focal neuronal current sources," *IEEE Trans. Med. Imaging*, vol. 16, pp. 338-348, 1997.
- [13] R. Grave de Peralta Menendez and S. L. Gonzalez Andino, "Distributed source models: standard solutions and new developments," In: Uhl, C. (ed): *Analysis of neurophysiological brain functioning*, Springer Verlag, pp. 176-201, 1998.
- [14] K. Sekihara and B. Scholz, "Average-intensity reconstruction and Wiener reconstruction of bioelectric current distribution based on its estimated covariance matrix," *IEEE Trans. Biomed. Eng.*, vol. 42, pp. 149-157, 1995.
- [15] J. Hori, T. Miwa, T. Ohshima, and B. He, "Cortical dipole imaging of movement-related potentials by means of parametric inverse filters incorporating with signal and noise covariance," *Methods Inf. Med.*, 2007.
- [16] P.C. Hansen, "Truncated singular value decomposition solutions to discrete ill-posed problems with ill-determined numerical rank," *SIAM J. Sci. Stat. Comput.*, vol.11, pp.503-518, 1990.
- [17] A.N. Tikhonov and V.Y. Arsenin, "Solutions of illization of brain electrical activity via linearly constrained minimum variance spatial filtering," *IEEE Trans. Biomed. Eng.*, vol.44, pp.867-880, 1997.
- [18] A. Hyvarinen, "Fast and robust fixed-point algorithms for independent component analysis," *IEEE Trans. Neural Networks*, vol.13, pp.411-430, 2000.